Discontinuous Galerkin Isogeometric Analysis for Elliptic Problems with Discontinuous Coefficients on Surfaces

Article *in* Numerical Algorithms · November 2020

DOI: 10.1007/s11075-019-00856-x

CITATIONS
0

READS
150

1 author:

Stephen Edward Moore
University of Cape Coast
13 PUBLICATIONS **166** CITATIONS

SEE PROFILE

Discontinuous Galerkin Isogeometric Analysis for Elliptic Problems with Discontinuous Diffusion Coefficients on Surfaces

Stephen Edward Moore

Department of Mathematics,
University of Cape Coast, Ghana.
stephen.moore@ucc.edu.gh

Abstract. This paper is concerned with using discontinuous Galerkin isogeometric analysis (dG-IGA) as a numerical treatment of Diffusion problems on orientable surfaces $\Omega \subset \mathbb{R}^3$. The computational domain or surface considered consist of several non-overlapping sub-domains or patches which are coupled via an interior penalty scheme. In Langer and Moore [13], we presented *a priori* error estimate for conforming computational domains with matching meshes across patch interface and a constant diffusion coefficient. However, in this article, we generalize the *a priori* error estimate to non-matching meshes and discontinuous diffusion coefficients across patch interfaces commonly occurring in industry. We construct B-Spline or NURBS approximation spaces which are discontinuous across patch interfaces. We present *a priori* error estimate for the symmetric discontinuous Galerkin scheme and numerical experiments to confirm the theory.

Key words: discontinuous Galerkin, multipatch isogeometric analysis, elliptic problems, *a priori* error analysis, surface PDE, interior penalty Galerkin, Laplace-Beltrami, discontinuous coefficients.

1 Introduction

In this paper, we consider the second-order elliptic boundary value problem on a open, smooth, connected and oriented two dimensional surface $\Omega \subset \mathbb{R}^3$ as follows: find $u : \overline{\Omega} \to \mathbb{R}$ such that

$$-\mathrm{div}_\Omega(\alpha \nabla_\Omega u) + u = f \text{ in } \Omega, \quad u = 0 \text{ on } \Gamma_D, \quad \mathbf{n} \cdot (\alpha \nabla_\Omega u) = g_N \text{ on } \Gamma_N, \tag{1.1}$$

where the diffusion coefficient α is uniformly bounded i.e. $\alpha_{min} \leq \alpha \leq \alpha_{max}$ with positive constants α_{max} and α_{min}, f and g_N are given sufficiently smooth data. The physical or computational domain $\Omega \subset \mathbb{R}^3$ is compact, connected and positively oriented surface with boundary $\partial\Omega$. The boundary of the computational domain consists of the Dirichlet part Γ_D with positive boundary measure and a Neumann part Γ_N such that $\partial\Omega := \Gamma_D \bigcup \Gamma_N$. The operators div_Ω and ∇_Ω are the surface divergence and surface gradient respectively, and will be defined in Section 2.

Partial Differential Equations (PDEs) on surfaces arise in many fields of application like material science, fluid mechanics, electromagnetics, biology and image processing, see e.g.[7] for several interesting discussions on applications. For several years, numerical methods dedicated to the solutions of PDEs on manifolds including conforming and non-conforming finite element methods (FEM) have been well studied and applied to compute the solution of elliptic and parabolic evolution problems on fixed and evolving computational domains, see,

e.g., [7, 5]. We note that there are however some drawbacks to the standard surface FEM. The standard surface FEM has two main sources of error: the error due to the approximation of the infinite dimensional spaces with finite dimensional spaces in the variational problem and the geometric error resulting from the approximation of the surface. These drawbacks are due to the discrete variational formulation of the PDE that is constructed on a triangulated surface which contains the finite elements space as discussed by Dzuik and Elliott in [7].

As an alternative aproach to the surface FEM, we resort to Isogeometric Analysis (IGA). The numerical scheme is based on B-splines and Non-Uniform B-splines (NURBS) and was proposed to approximate solutions of PDEs, see e.g. [10]. The method uses the same class of basis functions for representing both the geometry of the computational domain and also approximating the solution of problems modeled by PDEs. By using the exact representation of the geometry, the geometrical errors introduced by approximation of computational domains in the surface FEM are eliminated. This is especially of importance in the discretization of PDEs on surfaces. However, we note that IGA can also have geometry-related failures such as holes, singularities, etc. see e.g.[19]. Such failures or features are beyond the scope of this article. IGA uses B-splines or Non-Uniform Rational B-Splines (NURBS) basis functions which are standard in Computer Aided Design (CAD). The NURBS basis functions have several advantages making them suitable for analysis, see [10]. The mathematical analysis of the approximation properties, the stability and discretization error estimates of NURBS spaces and analysis of several refinement strategies, i.e., *h-p-k* refinements can be found in [2]. In many practical applications, the computational domains cannot be represented by a single B-spline or NURBS domain but by several patches or sub-domains. In this sense, single patch IGA and multi-patch IGA have been addressed in [3].

Alternatively, multi-patches can also be coupled via interior penalty Galerkin methods. In our earlier articles, see e.g., [13, 12, 16, 14], we analyzed the multi-patch discontinuous Galerkin IGA (dG-IGA) for diffusion and biharmonic problems and presented several convincing numerical results for conforming domains with matching meshes. However, in this paper, we will generalize the analysis to include non-matching meshes with jumping diffusion coefficients across patch boundaries and present *a priori* error estimates for diffusion problems. Our analysis follows the monograph [6] and requires three main ingredients; discrete stability, consistency and boundedness of the discrete bilinear form. Then using the approximation estimates, see e.g., [2], we finally derive *a priori* error estimate. The linear system obtained from the discretization of the problem is solved by means of a preconditioned conjugate gradient (PCG) with a scaled Dirichlet preconditioner as presented in primal isogeometric tearing and interconnecting (dG-IETI-DP) see e.g., [9].

The rest of the paper is organized as follows; Section 2 gives a brief introduction to function spaces, weak formulation, NURBS surfaces and geometrical mappings and isogeometric analysis. We present the dG-IGA scheme in Section 3. In Section 4, we present the multi-patch dG-IGA and the analysis of the dG-IGA scheme. The *a priori* error estimate is presented in Section 5. We present numerical results for an open surface and a closed surface with non-matching meshes respect to the jumping diffusion coefficient in Section 6. Finally, we conclude and give an outlook.

2 Preliminaries

In this section, we introduce briefly introduce Sobolev spaces, NURBS surfaces and isogeometric analysis method, see e.g. [1, 10] for detailed study. Firstly, let the computational domain Ω be a compact smooth and oriented surface with boundary $\partial\Omega$. We introduce the Sobolev space $H^s(\Omega) := \{v \in L_2(\Omega) : D^\kappa v \in L_2(\Omega), \text{ for } 0 \leq |\kappa| \leq s\}$, where $L_2(\Omega)$ denote the space of square integrable functions and $\kappa = (\kappa_1, \ldots, \kappa_d)$ be a multi-index with non-negative integers $\kappa_1, \ldots, \alpha_d$, and $|\kappa| = \kappa_1 + \ldots + \kappa_d$, $D^\kappa := \partial^{|\kappa|}/\partial x^\kappa$. We associate the Sobolev space $H^s(\Omega)$ with the norm $\|v\|_{H^s(\Omega)} = \left(\sum_{0\leq|\kappa|\leq s} \|D^\kappa v\|^2_{L_2(\Omega)}\right)^{1/2}$.

The variational formulation of the surface diffusion problem (1.1) reads: find $u \in V_0$ such that

$$a(u, v) = \ell(v), \quad \forall v \in V_0, \tag{2.1}$$

where the bilinear and linear forms are given by

$$a(u, v) = \int_\Omega (\alpha \nabla_\Omega u \cdot \nabla_\Omega v + uv)\, dx \quad \text{and} \quad \ell(v) = \int_\Omega fv\, dx + \int_{\Gamma_N} g_N v\, ds, \tag{2.2}$$

with $V_0 := \{v \in H^1(\Omega) : v = 0 \quad \text{on} \quad \Gamma_D\}$. The existence and uniqueness of the solution of such a variational problem (2.1) follows the standard arguments of Lax-Milgram lemma if $u \in H^2(\Omega)$ satisfies

$$\|u\|_{H^2(\Omega)} \leq \|f\|_{L_2(\Omega)}, \tag{2.3}$$

see e.g. [18] for further details.

2.1 NURBS Geometrical Mapping and Surfaces

Let $\xi = (\xi_1, \xi_2) \in \mathbb{R}^2$ be a vector-valued independent variable in the parameter domain $\widehat{\Omega}$. By means of a smooth and invertible geometrical mapping Φ, the computational domain $\Omega \subset \mathbb{R}^3$ is defined as

$$\Phi : \widehat{\Omega} \to \Omega \subset \mathbb{R}^3, \quad \xi \to x = \Phi(\xi), \tag{2.4}$$

where the parameter domain $\widehat{\Omega} \subset \mathbb{R}^2$ as illustrated in Fig. 1.

We introduce briefly some important mathematical tools necessary for the analysis of surface PDEs. The following objects are obtained by means of the geometrical mapping (2.4) in the parameter domain. The Jacobian $\widehat{J}$, first fundamental form $\widehat{F}$ and the determinant $\widehat{g}$ of the geometrical mapping are respectively given by

$$\widehat{J} := \left[\frac{\partial \Phi_k}{\partial \xi_l}\right] \in \mathbb{R}^{3\times 2}, \quad k = 1, 2, 3,\ l = 1, 2, \tag{2.5}$$

$$\widehat{F}(\xi) = \left(\widehat{J}(\xi)\right)^T \widehat{J}(\xi) \in \mathbb{R}^{2\times 2} \quad \text{and} \quad \widehat{g}(\xi) = \sqrt{\det\left(\widehat{F}(\xi)\right)} \in \mathbb{R}. \tag{2.6}$$

Next, we present some differential operators by using notations in the parameter domain. We consider a smooth function ϕ defined on the manifold Ω, by using the invertible geometrical mapping (2.4) to obtain

$$\phi(x) = \widehat{\phi}(\xi) \circ \Phi^{-1}(x), \quad x \in \Omega, \tag{2.7}$$

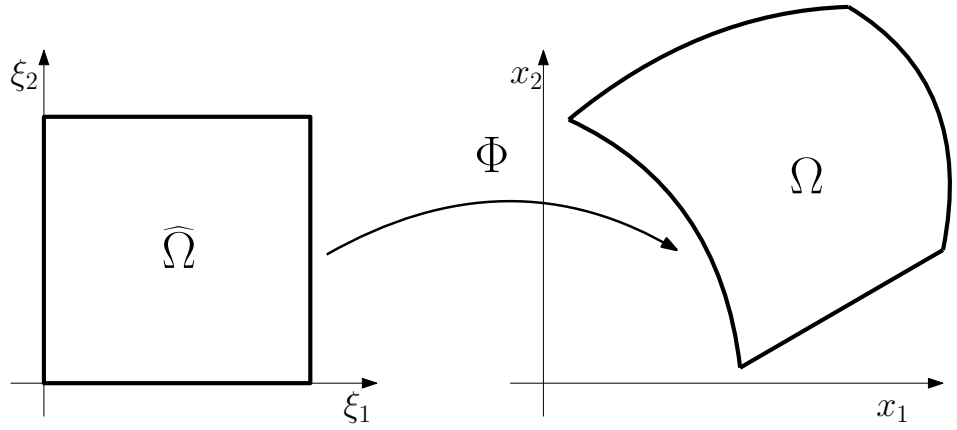

Fig. 1. Illustration of the geometrical map $\Phi : \widehat{\Omega} \subset \mathbb{R}^2 \to \Omega \subset \mathbb{R}^3$ for a patch.

where $\widehat{\phi}(\xi) = \phi(\Phi(\xi))$. Using the gradient operator in the parameter space $\nabla\widehat{\phi}$, the tangential gradient of the manifold is given by

$$\nabla_\Omega \phi(x) := \widehat{J}(\xi)\widehat{F}^{-1}(\xi)\nabla\widehat{\phi}(\xi) \circ \Phi^{-1}(x). \tag{2.8}$$

The divergence operator for the vector-valued function can be written as

$$\nabla_\Omega \cdot \phi(x) := \frac{1}{\widehat{g}\xi)}\nabla \cdot \left[\widehat{g}(\xi)\widehat{F}^{-1}(\xi)\widehat{J}^T(\xi)\widehat{\phi}(\xi)\right] \circ \Phi^{-1}(x). \tag{2.9}$$

The Laplace-Beltrami operator on the manifold Ω is defined for a twice continuously differentiable function $\phi : \Omega \to \mathbb{R}$ as

$$\Delta_\Omega \phi(x) = \frac{1}{\widehat{g}(\xi)}\nabla \cdot \left[\widehat{g}(\xi)\widehat{F}^{-1}(\xi)\nabla\widehat{\phi}(\xi)\right] \circ \Phi^{-1}(x). \tag{2.10}$$

The unit normal vector on the manifold $\Omega \subset \mathbb{R}^3$ is obtained by the geometrical mapping of

$$\widehat{\mathbf{n}}(\xi) := \frac{\widehat{t}_1(\xi) \times \widehat{t}_2(\xi)}{\|\widehat{t}_1(\xi) \times \widehat{t}_2(\xi)\|}, \tag{2.11}$$

where $\widehat{t}_l(\xi) := \partial\Phi(\xi)/\partial\xi_l$ is the tangent vector to a curve in $\mathbb{R}^3$ with $l = 1, 2$. The manifold Ω has a tangent plane at ξ if the tangent vectors are linearly independent.

Finally, by means of the geometrical mapping (2.4), we can write the Jacobian, first fundamental form and the determinant on the computational domain Ω as follows

$$J(x) = \widehat{J}(\xi) \circ \Phi^{-1}(x), \quad F(x) = \widehat{F}(\xi) \circ \Phi^{-1}(x) \quad \text{and} \quad g(x) = \widehat{g}(\xi) \circ \Phi^{-1}(x). \tag{2.12}$$

2.2 NURBS and Isogeometric Analysis

We begin by introducing the univariate B-splines since they are usually the industry standard.Given positive integers p and n, we define a vector $\Xi := \{0 = \xi_1, \ldots, \xi_{n+p+1} = 1\}$ with a

non-decreasing sequence of real numbers in the unit interval or parameter domain $\widehat{\Omega} = [0,1]$ called a knot vector. Given $\Xi, p \geq 1$, and n the number of basis functions, the univariate B-spline functions are defined by the following recursion formula

$$\widehat{B}_{i,0}(\xi) = \begin{cases} 1 & \text{if} \quad \xi_i \leq \xi < \xi_{i+1}, \\ 0 & \text{else}, \end{cases}$$

$$\widehat{B}_{i,p}(\xi) = \frac{\xi - \xi_i}{\xi_{i+p} - \xi_i} \widehat{B}_{i,p-1}(\xi) + \frac{\xi_{i+p+1} - \xi}{\xi_{i+p+1} - \xi_{i+1}} \widehat{B}_{i+1,p-1}(\xi), \tag{2.13}$$

where a division by zero is defined to be zero. We note that a basis function of degree p is $(p-m)$ times continuously differentiable across a knot value with the multiplicity m. If all internal knots have the multiplicity $m = 1$, then B-splines of degree p are globally $(p-1)-$continuously differentiable.

The bivariate B-spline basis functions are tensor products of the univariate B-spline basis functions (2.13). Let $\Xi_k = \{\xi_{1,k}, \ldots, \xi_{n_k+p_k+1,k}\}$ be the knot vectors for every direction $k = 1, 2$. Let $\mathbf{i} := (i_1, i_2), \mathbf{p} := (p_1, p_2)$ and the set $\overline{\mathcal{I}} = \{\mathbf{i} = (i_1, i_2) : i_k = 1, 2, \ldots, n_k;\ k = 1, 2\}$ be multi-indicies. Then the tensor product B-spline basis functions are defined by

$$\widehat{B}_{\mathbf{i},\mathbf{p}}(\xi) := \prod_{k=1}^{2} \widehat{B}_{i_k,p_k}(\xi_k), \tag{2.14}$$

where $\xi = (\xi_1, \xi_2) \in \widehat{\Omega} = (0,1)^2$. The univariate and bivariate B-spline basis functions are defined in the parametric domain by means of the corresponding B-spline basis functions $\{\widehat{B}_{\mathbf{i},\mathbf{p}}\}_{\mathbf{i} \in \overline{\mathcal{I}}}$.

The distinct values $\xi_l, l = 1, \ldots, n$ of the knot vectors Ξ provides a partition of $(0,1)^2$ creating a mesh $\widehat{\mathcal{K}}_h$ in the parameter domain where $\widehat{K}$ is a mesh element. The computational domain is described by means of a geometrical mapping $\mathbf{\Phi}$ such that $\Omega = \mathbf{\Phi}(\widehat{\Omega})$ and

$$\mathbf{\Phi}(\xi) := \sum_{\mathbf{i} \in \overline{\mathcal{I}}} C_{\mathbf{i}} \widehat{B}_{\mathbf{i},\mathbf{p}}(\xi), \tag{2.15}$$

where $C_{\mathbf{i}}$ are the control points.

We define the basis functions in the computational domain by means of the geometrical mapping as $B_{\mathbf{i},\mathbf{p}} := \widehat{B}_{\mathbf{i},\mathbf{p}} \circ \mathbf{\Phi}^{-1}$ and the discrete function space by

$$\mathbb{V}_h = \text{span}\{B_{\mathbf{i},\mathbf{p}} : \mathbf{i} \in \overline{\mathcal{I}}\}. \tag{2.16}$$

Finally, the NURBS isogeometric analysis scheme reads as folows; Find $u_h \in \mathbb{V}_h$ such that

$$a(u_h, v_h) = \ell(v_h), \quad \forall v_h \in \mathbb{V}_h, \tag{2.17}$$

with $\mathbb{V}_h \subset V_0$.

However, for many practical applications, the physical domain Ω consists of non-overlapping domains $\Omega_i, i = 1, \ldots, N$ called subdomains denoted by $\mathcal{T}_h := \{\Omega_i\}_{i=1}^N$ such that $\overline{\Omega} = \bigcup_{i=1}^N \overline{\Omega}_i$ and $\Omega_i \cap \Omega_j = \emptyset$ for $i \neq j$. Each patch is the image of an associated geometrical mapping $\mathbf{\Phi}_i$ such that $\mathbf{\Phi}_i(\widehat{\Omega}) = \Omega_i, i = 1, \ldots, N$, see Fig. 2. We denote by $F_{ij} = \partial\Omega_i \cap \partial\Omega_j, i \neq j$, the interior facets of two patches see Fig. 3. We assume the $F_{ij} \subset \partial\Omega_i$ for the interior facets. Let $F_i = \partial\Omega_i \cap \partial\Omega$ denote an edge of $\partial\Omega_i$. $\mathcal{F} := \mathcal{F}_I \cup \mathcal{F}_D$. We assume that for each patch $\Omega_i, i = 1, \ldots, N$, the underlying mesh $\mathcal{K}_{h,i}$ is quasi-uniform i.e. $h_K \leq h_i \leq C_u h_K$, for all $K \in \mathcal{K}_{h,i}, \quad i = 1, \ldots, N$, where $C_u \geq 1$ and $h_i = \max\{h_K, K \in \mathcal{K}_{h,i}\}$ is the mesh size of Ω_i and h_K is the diameter of of the mesh element K see e.g. [15].

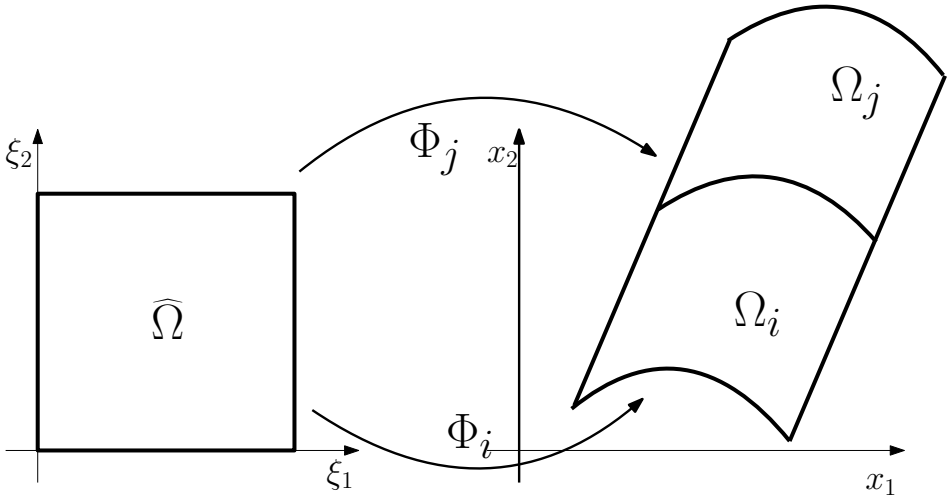

Fig. 2. Illustration of the multi-patch isogeometric analysis map $\Phi_i(\widehat{\Omega}) = \Omega_i$ and $\Phi_j(\widehat{\Omega}) = \Omega_j, i \neq j$.

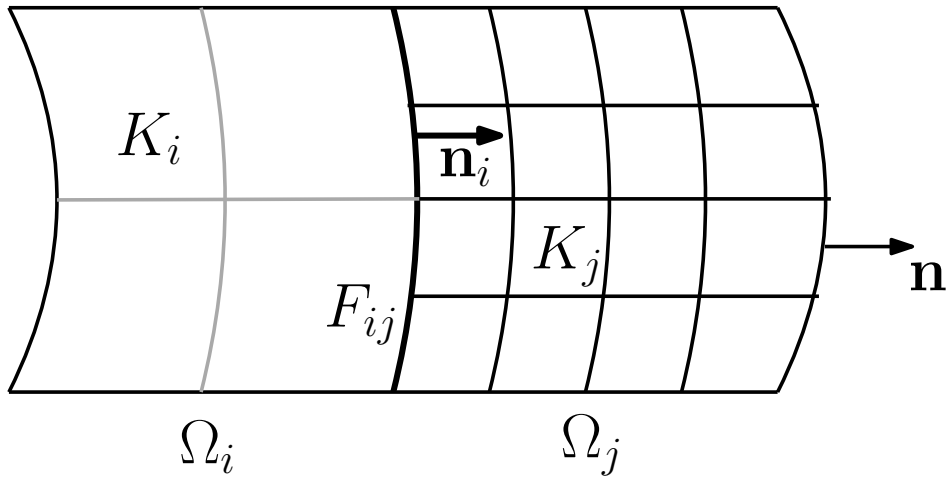

Fig. 3. Illustration of the underlying non-matching mesh of the multi-patch isogeometric

3 Discontinuous Galerkin IGA Scheme formulation

We recall some function spaces required for the derivation of interior penalty Galerkin schemes. We assign to each patch Ω_i a a real number s_i and collect them in the vector $\mathbf{s} = \{s_1, \ldots, s_N\}$. Let us now define the broken Sobolev space

$$H^{\mathbf{s}}(\Omega, \mathcal{T}_h) := \{v \in L_2(\Omega) : v|_{\Omega_i} \in H^{s_i}(\Omega_i),\ i = 1, \ldots, N\}, \tag{3.1}$$

and the corresponding broken Sobolev norm and semi-norm

$$\|v\|_{H^{\mathbf{s}}(\Omega,\mathcal{T}_h)} := \left(\sum_{i=1}^{N} \|v\|^2_{H^{s_i}(\Omega_i)}\right)^{1/2} \quad \text{and} \quad |v|_{H^{\mathbf{s}}(\Omega,\mathcal{T}_h)} := \left(\sum_{i=1}^{N} |v|^2_{H^{s_i}(\Omega_i)}\right)^{1/2}, \tag{3.2}$$

respectively.

We denote the restrictions of the function v on patches Ω_i and Ω_j, by v_i and v_j respectively. For the interior facets $F_{ij} \subset \partial\Omega_i$, let $\mathbf{n}_i$ be the outward unit normal vector with respect to Ω_i, which coincides with the outward unit normal $\mathbf{n}$ on $\partial\Omega$, see Fig. 3. We define the jump and average across the interior facets F_{ij} of a smooth function $v \in H^1(\Omega, \mathcal{T}_h)$ by

$$[\![v]\!] := v_i - v_j, \quad \textit{and} \quad \{v\} := \frac{1}{2}\left(v_i + v_j\right), F_{ij} \in \mathcal{F}_I, \tag{3.3}$$

whereas the jump and average functions on the facets F_i are given by $[\![v]\!] := v_i$, and $\{v\} := v_i$. Now, we present the dG-IGA variational scheme as follows: find $u \in V = H^{1+\mathbf{s}}(\Omega, \mathcal{T}_h)$ with $\mathbf{s} \in (1/2, 1]$, such that

$$a_h(u, v) = \ell_h(v), \quad \forall v \in V, \tag{3.4}$$

where the dG bilinear and linear forms considered throughout this paper are defined by the relationships where the bilinear form is given as

$$a_h(u, v) = \sum_{i=1}^{N} \big(a_i(u, v) + s_i(u, v) + p_i(u, v)\big), \tag{3.5}$$

with

$$\begin{aligned}
a_i(u, v) &:= \int_{\Omega_i} \alpha_i \nabla_\Omega u \cdot \nabla_\Omega v + uv \; dx, \\
s_i(u, v) &:= \sum_{F_{ij} \subset \partial\Omega_i} \int_{F_{ij}} \frac{\alpha_{ij}}{2} \Big(\{\nabla_\Omega u\}[\![v]\!] + \{\nabla_\Omega v\}[\![u]\!] \Big) \, ds, \\
p_i(u, v) &:= \sum_{F_{ij} \subset \partial\Omega_i} \int_{F_{ij}} \frac{\delta\alpha_{ij}}{2h_{ij}} [\![u]\!][\![v]\!] \, ds,
\end{aligned}$$

where δ is a non-zero positive real number. We have used a harmonic mean for the edges on the interface i.e. $h_{ij} = 2h_ih_j/(h_i + h_j)$ with $h_{ij} \leq 2h_i$ and $h_{ij} \leq 2h_j$ and similarly for the diffusion coefficient i.e. $\alpha_{ij} = 2\alpha_i\alpha_j/(\alpha_i + \alpha_j)$ with $\alpha_{ij} \leq 2\alpha_i$ and $\alpha_{ij} \leq 2\alpha_j$. The linear form is given by

$$\ell_h(v) = \sum_{i=1}^{N} \Big(\int_{\Omega_i} fv \, dx + \int_{F_i \in \mathcal{F}_N} g_N v \, ds \Big), \tag{3.6}$$

where $\mathcal{F}_N$ is the collection of all edges on the Neumann Boundary parts.

Remark 1. The choice of the penalty parameter δ depends on B-spline or NURBS degree p and the dimension of the computational domain $\Omega \subset \mathbb{R}^d$, for example $\delta = 2(p+1)(p+d)/d$ in the finite element theory, see, e.g. [17].

4 Analysis of the dG-IGA Scheme

For each subdomain $\Omega_i, i = 1, \ldots, N$, we will consider the discrete space $\mathbb{V}_{h,i}, i = 1, \ldots, N$ where $\mathbb{V}_h$ is given by (2.16). We define the discrete space corresponding to the domain Ω as

$$V_h := \{v \in \mathbb{V}_{h,i}, i = 1, \ldots, N\},$$

which allows discontinuities across the patch interface. The discrete dG-IGA scheme then reads as: find $u_h \in V_h$ such that

$$a_h(u_h, v_h) = \ell_h(v_h), \quad \forall v_h \in V_h. \tag{4.1}$$

The existence and uniqueness of the bilinear form $a_h(\cdot,\cdot)$ follow the popular Lax-Milgram theorem by showing the coercivity and boundedness. Next, we show that the bilinear form $a_h(\cdot,\cdot)$ is V_h-coercive with respect to the dG-norm

$$\|v\|_h^2 := \sum_{i=1}^{N} \left(\alpha_i \|\nabla_\Omega v_i\|_{L_2(\Omega_i)}^2 + \|v\|_{L_2(\Omega_i)}^2 + \sum_{F_{ij} \subset \partial\Omega_i} \frac{\delta\alpha_{ij}}{2h_{ij}} \|[\![v]\!]\|_{L_2(F_{ij})}^2 \right). \tag{4.2}$$

Remark 2. The discrete norm $\|\cdot\|_h$ from (4.2) is a norm on V_h. Indeed, if $\|v\|_h = 0$ for some function $v \in V_h$, then $\nabla_\Omega v = 0$ in each subdomain Ω_i. This means that the function v is a constant on each patch Ω_i, $i = 1, \ldots, N$. Furthermore, $\|v\|_h = 0$ yields that $[\![v]\!] = 0$ across the internal facets $F_{ij} \subset \partial\Omega_i$ are zero, i.e., v is constant in $\overline{\Omega}$. Finally, $v_i = 0$ on the boundary $\partial\Omega$ implies that this constant must be zero. Thus, $v = 0$ in $\overline{\Omega}$. The other norm axioms are obviously fulfilled.

To analyze the multi-patch interior penalty Galerkin scheme, the following discrete inverse and trace inequalities are required.

Lemma 1. *Let $v \in V_h$, then the following inverse inequalities hold;*

$$\|\nabla v\|_{L_2(\Omega_i)} \leq C_{inv,1,u} h_i^{-1} \|v\|_{L_2(\Omega_i)}, \tag{4.3}$$

and

$$\|v\|_{L_2(\partial\Omega_i)} \leq C_{inv,0,u} h_i^{-1/2} \|v\|_{L_2(\Omega_i)}, \tag{4.4}$$

where $C_{inv,1,u}$ and $C_{inv,0,u}$ are positive constants, which are independent of h_i and Ω_i.

We conclude with the continuous trace inequality,

Lemma 2. *Let $\Omega_i = \Phi_i(\widehat{\Omega})$ for $i = 1, \ldots, N$. Then the patch-wise scaled trace inequality*

$$\|v\|_{L_2(\partial\Omega_i)} \leq C_{t,u} h_i^{-1/2} \left(\|v\|_{L_2(\Omega_i)} + h_i^{1/2+\epsilon} |v|_{H^{1/2+\epsilon}(\Omega_i)} \right), \tag{4.5}$$

holds for all $v \in H^{1/2+\epsilon}(\Omega_i), \epsilon \in (0, 1/2]$, where h_i denotes the maximum mesh size in the physical domain, and $C_{t,u}$ is a positive constant that only depends on the shape regularity of the mapping Φ_i.

The proofs of Lemma 1 and Lemma 2 follows the standard procedure see e.g., [8] and [15]. from the Finite Element.

Lemma 3. *For an arbitrary positive ε and for $F_{ij} \subset \partial\Omega_i$ the estimates*

$$\left| \int_{F_{ij}} \frac{\alpha_{ij}}{2} \mathbf{n}_i \cdot \nabla_\Omega v_{h,i} [\![v_h]\!] \, ds \right| \leq \left(\alpha_i \varepsilon \|\nabla_\Omega v_{h,i}\|_{L_2(\Omega_i)}^2 + \frac{C_{inv,0,u}^2 \alpha_{ij}}{2\varepsilon h_{ij}} \|[\![v_h]\!]\|_{L_2(F_{ij})}^2 \right), \tag{4.6}$$

holds for all $v_{h,i}, v_{h,j} \in V_h$, a positive constant $C_{inv,0,u}$ and $\alpha_i > 0$.

Proof. Following the Cauchy Schwarz inequality, since $F_{ij} \subset \partial\Omega_i$, by using the trace inequality (4.4), we have

$$\begin{aligned}\left| \int_{F_{ij}} \frac{\alpha_{ij}}{2} \mathbf{n}_i \cdot \nabla_\Omega v_{h,i} [\![v_h]\!] \, ds \right| &\leq \frac{\alpha_{ij}}{2} ||\nabla_\Omega v_{h,i}||_{L_2(F_{ij})} ||[\![v_h]\!]||_{L_2(F_{ij})} \\ &\leq C_{inv,0,u} \frac{\alpha_{ij}}{2h_i^{1/2}} ||\nabla_\Omega v_{h,i}||_{L_2(\Omega_i)} ||[\![v_h]\!]||_{L_2(F_{ij})} \\ &\leq \frac{C_{inv,0,u}\alpha_{ij}}{h_{ij}^{1/2}} ||\nabla_\Omega v_{h,i}||_{L_2(\Omega_i)} ||[\![v_h]\!]||_{L_2(F_{ij})} \\ &\leq \left(\frac{\alpha_{ij}\varepsilon}{2} \|\nabla_\Omega v_{h,i}\|^2_{L_2(\Omega_i)} + \frac{C^2_{inv,0,u}\alpha_{ij}}{2\varepsilon h_{ij}} \|[\![v_h]\!]\|^2_{L_2(F_{ij})} \right),\end{aligned}$$

where we use $h_{ij} \leq 2h_i$ and $\alpha_{ij} \leq 2\alpha_i$, together with the inequality $ab \leq \varepsilon a^2/2 + b^2/(2\varepsilon), \forall a, b \in \mathbb{R}$ with $\varepsilon > 0$ to complete the proof. □

Using the above result, we proceed to show the coercivity of the bilinear form $a_h(\cdot,\cdot)$.

Lemma 4 (Coercivity). *Let $a_h(\cdot,\cdot) : V_h \times V_h \to \mathbb{R}$ be the bilinear form (3.5). There exists $\delta_0 > 0$ and $\mu_c > 0$ such that $\delta > \delta_0$ and the discrete bilinear form $a_h(\cdot,\cdot)$ is V_h-coercive with respect to the norm $\|\cdot\|_h$, i.e.*

$$a_h(v_h, v_h) \geq \mu_c \|v_h\|_h^2, \quad \forall v_h \in V_h, \tag{4.7}$$

where μ_c is independent of α_i, h_i and N.

Proof. By using Cauchy-Schwarz's inequality, we proceed as follows

$$a_h(v_h, v_h) = \|v_h\|_h^2 - 2\sum_{i=1}^{N} \Big(\sum_{F_{ij} \subset \partial\Omega_i} \int_{F_{ij}} \frac{\alpha_{ij}}{2} \{\nabla_\Omega v_h\} [\![v_h]\!] \, ds \Big).$$

Using Cauchy Schwarz's inequality and Lemma 3, we have

$$a_h(v_h, v_h) \geq \Big(1 - \frac{\varepsilon}{2}\Big) \sum_{i=1}^{N} \alpha_i \|\nabla_\Omega v_{h,i}\|^2_{L_2(\Omega_i)} + \left(\delta - \frac{C^2_{inv,0,u}}{\varepsilon} \right) \sum_{i=1}^{N} \sum_{F_{ij} \subset \partial\Omega_i} \frac{\alpha_{ij}}{2h_{ij}} \|[\![v_h]\!]\|^2_{L_2(F_{ij})}.$$

For example, for $\mu_c = 1/2$, we choose $\varepsilon = 1$ and $\delta \geq C^2_{inv,0,u}$. □

Next, we prove the uniform boundedness for the bilinear form $a_h(\cdot,\cdot)$ on $V_{h,*} \times V_h$, where $V_{h,*} = V_0 \cap H^{1+\mathbf{s}}(\Omega, \mathcal{T}_h) + V_h$ with $\mathbf{s} > 1/2$ is equipped with the norm

$$\|v\|_{h,*} = \left(\|v\|_h^2 + \sum_{i=1}^{N} \alpha_i h_i \|\nabla_\Omega v_i\|^2_{L_2(\partial\Omega_i)} \right)^{1/2}. \tag{4.8}$$

To prove *a priori* estimates, we need the following two auxiliary lemmata to proof for the boundedness of the bilinear form.

Lemma 5. *For a positive parameter δ and for $F_{ij} \subset \partial\Omega_i, i = 1, \ldots, N$ and diffusion coefficients α_i and α_{ij}, the estimates*

$$\left| \int_{F_{ij}} \frac{\alpha_{ij}}{2} \mathbf{n}_i \cdot \nabla_\Omega u_i [\![v_h]\!] \, ds \right| \leq \left(\frac{2\alpha_i h_i}{\delta} \|\nabla_\Omega u_i\|^2_{L_2(\partial\Omega_i)} \right)^{1/2} \left(\frac{\alpha_{ij}\delta}{2h_{ij}} \|[\![v_h]\!]\|^2_{L_2(F_{ij})} \right)^{1/2}, \tag{4.9}$$

$$\left| \int_{F_{ij}} \frac{\alpha_{ij}}{2} \mathbf{n}_i \cdot \nabla_\Omega v_{h,i} [\![u]\!] \, ds \right| \leq \left(\frac{2C^2_{inv,0,u}\alpha_i}{\delta} \|\nabla_\Omega v_{h,i}\|^2_{L_2(\Omega_i)} \right)^{1/2} \left(\frac{\alpha_{ij}\delta}{2h_{ij}} \|[\![u]\!]\|^2_{L_2(F_{ij})} \right)^{1/2}, \tag{4.10}$$

hold for all $u \in V_{h,*}$ and for all $v_h \in V_h$.

Proof. For $F_{ij} \subset \partial\Omega_i$, using Cauchy-Schwarz's inequality, we obtain

$$\left| \int_{F_{ij}} \frac{\alpha_{ij}}{2} \mathbf{n}_i \cdot \nabla_\Omega u_i [\![v_h]\!] \, ds \right| \leq \left(\frac{\alpha_{ij} h_{ij}}{2\delta} \|\nabla_\Omega u_i\|^2_{L_2(\partial\Omega_i)} \right)^{\frac{1}{2}} \left(\frac{\alpha_{ij}\delta}{2h_{ij}} \|[\![v_h]\!]\|^2_{L_2(F_{ij})} \right)^{\frac{1}{2}}.$$

We conclude the proof since $h_{ij} \leq 2h_i$ and $\alpha_{ij} \leq 2\alpha_i$ For the second inequality, we apply the Cauchy Schwarz inequality to obtain

$$\left| \int_{F_{ij}} \frac{\alpha_{ij}}{2} \mathbf{n}_i \cdot \nabla_\Omega v_{h,i} [\![u]\!] \, ds \right| \leq \left(\frac{\alpha_{ij} h_{ij}}{2\delta} \|\nabla_\Omega v_{h,i}\|^2_{L_2(\partial\Omega_i)} \right)^{\frac{1}{2}} \left(\frac{\alpha_{ij}\delta}{2h_{ij}} \|[\![u]\!]\|^2_{L_2(F_{ij})} \right)^{\frac{1}{2}}.$$

Since $h_{ij} \leq 2h_i$ and $\alpha_{ij} \leq 2\alpha_i$, by applying the inequality (4.4) for $v_{h,i} \in V_h$, we complete the proof. □

Next, we proceed with the boundedness of the bilinear form $a_h(\cdot, \cdot)$ as follows ;

Lemma 6 (Boundedness). *The discrete bilinear form $a_h(\cdot, \cdot)$ is uniformly bounded on $V_{h,*} \times V_h$, i.e. there exists a mesh-independent positive constant μ_b such that*

$$|a_h(u, v_h)| \leq \mu_b \|u\|_{h,*} \|v_h\|_h, \forall u \in V_{h,*}, \forall v_h \in V_h. \tag{4.11}$$

Proof. The first term of the bilinear form (3.5) is estimated using Cauchy-Schwarz's inequality as follows

$$\left| \sum_{i=1}^N a_i(u, v_h) \right| \leq \left(\sum_{i=1}^N \alpha_i \|\nabla_\Omega u\|^2_{L_2(\Omega_i)} \right)^{\frac{1}{2}} \left(\sum_{i=1}^N \alpha_i \|\nabla_\Omega v_h\|^2_{L_2(\Omega_i)} \right)^{\frac{1}{2}}. \tag{4.12}$$

Using Cauchy Schwarz's inequality together with Lemma 5, the second term yields

$$\begin{aligned} \left| \sum_{i=1}^N s_i(u, v_h) \right| \leq & \left(\sum_{i=1}^N \sum_{F_{ij} \subset \partial\Omega_i} \left[\frac{2\alpha_i h_i}{\delta} \|\nabla_\Omega u\|^2_{L_2(\partial\Omega_i)} + \frac{\delta\alpha_{ij}}{2h_{ij}} \|[\![u]\!]\|_{L_2(F_{ij})} \right] \right)^{\frac{1}{2}} \\ & \times \left(\sum_{i=1}^N \sum_{F_{ij} \subset \partial\Omega_i} \frac{2C^2_{inv,0,u}\alpha_i}{\delta} \|\nabla_\Omega v_h\|^2_{L_2(\Omega_i)} + \frac{\delta\alpha_{ij}}{2h_{ij}} \|[\![v_h]\!]\|_{L_2(F_{ij})} \right)^{\frac{1}{2}}. \end{aligned} \tag{4.13}$$

Also, the last term of the bilinear form is estimated by applying Cauchy-Schwarz's inequality to obtain

$$\left| \sum_{i=1}^N p_i(u, v_h) \right| \leq \left(\sum_{i=1}^N \sum_{F_{ij} \subset \partial\Omega_i} \frac{\delta\alpha_{ij}}{2h_{ij}} \|[\![u]\!]\|^2_{L_2(F_{ij})} \right)^{\frac{1}{2}} \left(\sum_{i=1}^N \sum_{F_{ij} \subset \partial\Omega_i} \frac{\delta\alpha_{ij}}{2h_{ij}} \|[\![v_h]\!]\|^2_{L_2(F_{ij})} \right)^{\frac{1}{2}}. \tag{4.14}$$

Combining all the terms (4.12) – (4.14), we conclude the proof with the positive constant $\mu_b = 2\sqrt{\max\{1, (1 + C_{inv,0,1}^2/\delta)\}}$. □

We note that the discrete norms $\|\cdot\|_h$ and $\|\cdot\|_{h,*}$ are uniformly equivalent on the dicrete space V_h. In the next lemma, we present this equivalence of the discrete norms since the convergence analysis is considered in the discrete norm $\|\cdot\|_h$.

Lemma 7. *The norms $\|\cdot\|_h$ and $\|\cdot\|_{h,*}$ are uniformly equivalent on the discrete space V_h such that*

$$C_e\|v_h\|_{h,*} \leq \|v_h\|_h \leq \|v_h\|_{h,*}, \quad \forall v_h \in V_h, \tag{4.15}$$

where C_e is mesh independent.

Proof. The proof of the upper bound follows immediately. However, the proof of the lower bound follows by using the definition of the norm (4.8) together with the trace inequality (4.4) with $C_e = \left(1 + C_{inv,0,1}^2/\delta\right)^{-1}$. □

A consequence of Lemma 7 yields the boundedness of the bilinear form $a_h(\cdot,\cdot)$ with a positive constant $\tilde{\mu}_b$ as follows

$$|a_h(u_h, v_h)| \leq \tilde{\mu}_b\|u_h\|_h\|v_h\|_h, \quad \forall u_h, v_h \in V_h, \tag{4.16}$$

where $\tilde{\mu}_b = \mu_b \left(1 + C_{inv,0,1}^2/\delta\right)^{-1/2}$.

5 Error Analysis of dG-IGA Discretization

Finally, we present the approximation estimates required to obtain *a priori* error estimates. For patch $\Omega_i, i = 1, \ldots, N$, let $\Pi_{h,i} : L_2(\Omega_i) \to \mathbb{V}_{h,i}$ denote a quasi-interpolant that yields optimal approximation results. Of course, such an interpolant is known to exist and has been well studied and presented in [2, 3] as follows

Lemma 8. *Let l and s be integers with $0 \leq l \leq s \leq p+1$ and $K \in \mathcal{K}_{h,i}$. Then there exist an interpolant $\Pi_{h,i}v \in \mathbb{V}_{h,i}$ for all $v \in H^s(\Omega_i)$ and a constant $C_s > 0$ such that the following inequality holds*

$$\sum_{K\in\mathcal{K}_{h,i}} |v - \Pi_{h,i}v|_{H^l(K)}^2 \leq C_s h_i^{2(s-l)}\|v\|_{H^s(\Omega_i)}^2, \tag{5.1}$$

where h_i is the mesh size in the physical domain, and p denotes the underlying polynomial degree of the B-spline or NURBS.

For patch $\Omega_i, i = 1, \ldots, N$, the local estimate (5.1) yields a global estimate if the multiplicity of the inner knots is not larger than $p + 1 - l$ and $\Pi_{h,i}v \in \mathbb{V}_{h,i} \cap H^l(\Omega_i)$.

Proposition 1. *Let $v \in H^s(\Omega_i)$ be a function defined in the physical domain Ω_i. Given an integer l such that $0 \leq l \leq p+1, l \leq s$, and $p \leq s+1$, where s is the smoothness of the considered B-Spline basis. Then there exists a projection operator $\Pi_{h,i} : L_2(\Omega_i) \to \mathbb{V}_{h,i}$ such that the approximation error estimates*

$$|v - \Pi_{h,i}v|_{H^l(\Omega_i)} \leq C_s h_i^{(\beta-l)}\|v\|_{H^{s_i}(\Omega_i)}, \tag{5.2}$$

where $\beta = \min\{p+1, l\}$, h_i denotes the maximum mesh-size parameter in the physical domain and the generic constant C_s only depends on l, s and p, the shape regularity of the physical domain Ω_i described by the mapping Φ and, in particular, $\nabla_\Omega \Phi$.

Proof. See [4, Proposition 3.2].

For the error analysis, we assume that the patches have the same regularity such that $\mathbf{s} = \{s_1, s_2, \ldots, s_N\} = s$ and $H^{1+s}(\Omega_i), i = 1, \ldots, N$.

Lemma 9. *Let $v \in V_0 \cap H^{1+s}(\Omega_i)$ with $s > 1/2$ and $p \geq 1$. By assuming quasi-uniform meshes, then there exists a projection $\Pi_h v \in V_h$ and generic positive constants C_0 and C_1 such that the following error estimates hold*

$$\sum_{i=1}^{N} \sum_{F_{ij} \subset \partial\Omega_i} \frac{\delta \alpha_{ij}}{2h_{ij}} \|[\![v - \Pi_h v]\!]\|^2_{L_2(F_{ij})} \leq C_0 \sum_{i=1}^{N} \left(h_i^{2r} + \sum_{F_{ij} \subset \partial\Omega_i} \frac{h_j}{h_i} h_j^{2r} \right) \alpha_i \|v\|^2_{H^{1+r}(\Omega_i)}, \tag{5.3}$$

$$\sum_{i=1}^{N} \alpha_i h_i \|\nabla_\Omega (v - \Pi_h v)\|^2_{L_2(\partial\Omega_i)} \leq C_1 \sum_{i=1}^{N} \alpha_i h_i^{2r-1} \|v\|^2_{H^{1+r}(\Omega_i)}, \tag{5.4}$$

where $r = \min\{s, p\}$, the constant C_0 and C_1 Ω_i, are independent of h_i and h_j and $F_{ij} \subset \partial\Omega_i$ are the interior facets.

Proof. By using (3.3) with Lemma 2 and Proposition 1, we estimate the first term as follows

$$\begin{aligned}
\frac{\delta \alpha_{ij}}{2h_{ij}} \|v - \Pi_{h,i} v\|^2_{L_2(F_{ij})} &\leq \frac{\delta \alpha_{ij}}{2h_{ij}} C^2_{t,u} \left(h_i^{-1} \|v - \Pi_{h,i} v\|^2_{L_2(\Omega_i)} + h_i^{2\epsilon+1} |v - \Pi_{h,i} v|^2_{H^{1/2+\epsilon}(\Omega_i)} \right) \\
&\leq 2\delta C^2_{t,u} C_s \frac{\alpha_i}{2h_{ij}} \left(h_i^{-1} h_i^{2(1+r)-1/2+\epsilon} + h_i^{2\epsilon+1} h_i^{2r} \right) \|v\|^2_{H^{1+r}(\Omega_i)} \\
&\leq 4\delta C^2_{t,u} C_s \frac{\alpha_i}{2h_{ij}} h_i^{2r-1} \|v\|^2_{H^{1+r}(\Omega_i)}.
\end{aligned} \tag{5.5}$$

Similarly, the second term

$$\frac{\delta \alpha_{ij}}{2h_{ij}} \|v - \Pi_{h,j} v\|^2_{L_2(F_{ij})} \leq 4\delta C^2_{t,u} C_s \frac{\alpha_i}{2h_{ij}} h_j^{2r-1} \|v\|^2_{H^{1+r}(\Omega_j)}. \tag{5.6}$$

Now, we complete the proof by summing with respect to the interior facets $F_{ij} \subset \partial\Omega_i$ and $i = 1, 2, \ldots, N$, to obtain

$$\sum_{i=1}^{N} \sum_{F_{ij} \subset \partial\Omega_i} \frac{\delta \alpha_{ij}}{2h_{ij}} \|[\![v - \Pi_h v]\!]\|^2_{L_2(F_{ij})} \leq C_0 \sum_{i=1}^{N} \alpha_i \left(h_i^{2r} + \sum_{F_{ij} \subset \partial\Omega_i} \frac{h_j}{h_i} h_j^{2r} \right) \|v\|^2_{H^{1+r}(\Omega_i)}. \tag{5.7}$$

where $C_0 = \delta C^2_{t,u} C_s$. The proof of (5.4) follows by using Lemma 2 and the approximation estimate of Proposition 1 as follows

$$\begin{aligned}
\sum_{i=1}^{N} \alpha_i h_i \|\nabla_\Omega (v - \Pi_{h,i} v)\|^2_{L_2(\partial\Omega_i)} &\leq \sum_{i=1}^{N} \alpha_i C^2_{t,u} C_s \left(h_i^{2r} + h_i^{2\epsilon+1} h_i^{2(1+r-3/2-\epsilon)} \right) \|v\|^2_{H^{1+r}(\Omega_i)} \\
&\leq 2C_s C^2_{t,u} \sum_{i=1}^{N} \alpha_i h_i^{2r} \|v\|^2_{H^{1+r}(\Omega_i)},
\end{aligned} \tag{5.8}$$

where $C_1 = 2C_s C^2_{t,u}$. ∎

To derive the *a priori* error estimate, we show that the interpolant yields the optimal approximation estimate in the discrete norms.

Lemma 10. *Let $v \in V_0 \cap H^{1+s}(\Omega_i)$ with $s > 1/2$ and $p \geq 1$. Then there exists a projection $\Pi_h v \in V_h$ and generic positive constants C_2 and C_3 such that*

$$\|v - \Pi_h v\|_h^2 \leq C_2 \sum_{i=1}^{N} \left(h_i^{2r} + \sum_{F_{ij} \subset \partial\Omega_i} \frac{h_j}{h_i} h_j^{2r} \right) \alpha_i \|v\|_{H^{1+r}(\Omega_i)}^2, \tag{5.9}$$

$$\|v - \Pi_h v\|_{h,*}^2 \leq C_3 \sum_{i=1}^{N} \left(h_i^{2r} + \sum_{F_{ij} \subset \partial\Omega_i} \frac{h_j}{h_i} h_j^{2r} \right) \alpha_i \|v\|_{H^{1+r}(\Omega_i)}^2, \tag{5.10}$$

where $F_{ij} \subset \partial\Omega_i$ are the interior facets, of Ω_i, $r = \min\{s, p\}$ and C_2 and C_3 only depend on s and p.

Proof. Following from the definition of the discrete norms (4.2) and (4.8) together with Lemma 9, we complete the proof. □

Finally, we prove the main result in this section, namely *a priori* error estimate for surfaces. We will present the results for the discrete norm $\|\cdot\|_h$ and the $\|\cdot\|_{L_2(\Omega)}-$norm.

Theorem 1. *Let $u \in V_0 \cap H^{1+s}(\Omega_i)$ with $s > 1/2$ be the exact solution of the model (2.1) and $u_h \in V_h$ with $p \geq 1$ be the discrete solution of the dG-IGA scheme (4.1). For the penalty parameter δ chosen as in Lemma 4, then the discretization error estimate*

$$\|u - u_h\|_h^2 \leq C \sum_{i=1}^{N} \left(h_i^{2r} + \sum_{F_{ij} \subset \partial\Omega_i} \frac{h_j}{h_i} h_j^{2r} \right) \alpha_i \|u\|_{H^{1+r}(\Omega_i)}^2, \tag{5.11}$$

holds true, where $r = \min\{s, p\}$ and p denotes the underlying NURBS degree of the patch Ω_i, and C is a positive constant independent of the h_i and h_j.

Proof. By using the coercivity result Lemma 4, Galerkin orthogonality (5.12) and the boundedness of the discrete bilinear form, Lemma 6, we obtain

$$\begin{aligned} \mu_c \|\Pi_h u - u_h\|_h^2 \leq a_h(\Pi_h u - u_h, \Pi_h u - u_h) &= a_h(\Pi_h u - u, \Pi_h u - u_h) \\ &\leq \mu_b \|\Pi_h u - u\|_{h,*} \|\Pi_h u - u_h\|_h. \end{aligned} \tag{5.12}$$

Thus, we have

$$\|\Pi_h u - u_h\|_h^2 \leq (\mu_b/\mu_c)^2 \, \|\Pi_h u - u\|_{h,*}^2 \tag{5.13}$$

Using Lemma 9, we get

$$\begin{aligned} \|u - u_h\|_h^2 &\leq \|u - \Pi_h u\|_h^2 + \|\Pi_h u - u_h\|_h^2 \\ &\leq C_3 \sum_{i=1}^{N} \left(h_i^{2r} + \sum_{F_{ij} \subset \partial\Omega_i} \frac{h_j}{h_i} h_j^{2r} \right) \alpha_i \|u\|_{H^{1+r}(\Omega_i)}^2 \end{aligned}$$

$$+ (\mu_b/\mu_c)^2 C_4 \sum_{i=1}^{N} \left(h_i^{2r} + \sum_{F_{ij} \subset \partial\Omega_i} \frac{h_j}{h_i} h_j^{2r} \right) \alpha_i \|u\|^2_{H^{1+r}(\Omega_i)}$$

$$= C \sum_{i=1}^{N} \left(h_i^{2r} + \sum_{F_{ij} \subset \partial\Omega_i} \frac{h_j}{h_i} h_j^{2r} \right) \alpha_i \|u\|^2_{H^{1+r}(\Omega_i)},$$

where $C = \left(C_3 + (\mu_b/\mu_c)^2 C_4\right)$. Lemma 6. □

Remark 3. If, we assume matching meshes i.e. $h_i = h_j$, then the *a priori* error estimate (5.11) yields

$$\|u - u_h\|_h^2 \leq C \sum_{i=1}^{N} \alpha_i h_i^{2r} \|u\|^2_{H^{1+r}(\Omega_i)}, \tag{5.14}$$

which has been studied and presented in [13].

6 Numerical Results

In this section, we present numerical results for the dG-IGA scheme and *a priori* error estimate of Theorem 1. All the numerical experiments have been performed in G+SMO see [11]. We solve the linear system arising from the dG-IGA formulation by means a preconditioned conjugate gradient (PCG) algorithm with a scaled Dirichlet preconditioner where we choose vertex evaluation and edge averages as primal variables in the so-called dual-primal isogeometric tearing and interconnecting (dG-IETI-DP) solver. The solver is known to be robust with respect to diffusion coefficient see e.g. [9]. A reduction of the initial residual factor of 10^{-6} is used as a stopping criterion together with a zero initial guess. In the examples, we present non-matching grid of ratio $h_i/h_j = 2^q$, where q is the mesh refinement. The ratio h_i/h_j denotes the relative number of refinement on the neighboring patches and h_i, h_j are the maximum mesh sizes of patches Ω_i and Ω_j. The penalty parameter is chosen to be $\delta = 2(p+2)(p+1)$, where p is the NURBS degree. The convergence rate is computed using the formula $rate = \log_2 (e_i/e_{i+1})$, where $e_{i+1} = \|u - u_{h,i+1}\|_h$ and $e_i = \|u - u_{h,i}\|_h$ to study the discrete solution of the model problem. We consider as computational domains a quarter cylinder and a torus for the open and closed surfaces respectively, see Fig. 4.

6.1 Open Surface

We consider a diffusion problem with homogeneous Dirichlet boundary condition on an open surface Ω that is given by a quarter cylinder in the first quadrant i.e. $x \geq 0$ and $y \geq 0$ with unitary radius and height $L = 4$. The computational domain Ω is decomposed into 4 patches, with each of the patches having height of $L = 1$ and depicted by different color as seen on the left-hand side of Fig. 4 (left). The knot vectors representing the geometry of each patch are given by $\Xi_1 = \{0, 0, 0, 1, 1, 1\}$ and $\Xi_2 = \{0, 0, 1, 1\}$ in the ξ_1-direction and ξ_2-direction respectively. Let $f(\phi, z) = \varrho \left(\frac{\sigma^2\pi^2}{L^2} g_{\phi,1}(\phi) - g_{\phi,2}(\phi) \right) g_z(z)$, where $\phi := \arctan\left(\frac{x}{y}\right)$, $g_{\phi,1}(\phi) := (1 - \cos(\phi))(1 - \sin(\phi))$, $g_{\phi,2}(\phi) := (\cos(\phi) + \sin(\phi) - 4\sin(\phi)\cos(\phi))$, and $g_z(z) := \sin\left(\sigma\pi\frac{z}{L}\right)$ for $\sigma \in \mathbb{N}_0$ and $\varrho > 0$. The exact solution of the problem is $u(\phi, z) = \varrho g_{\phi,1}(\phi) g_z(z)$. In our numerical experiments, we set $\sigma = 3, \varrho = 1/\left(3/2 - \sqrt{2}\right)$. Fig. 5. We present the convergence

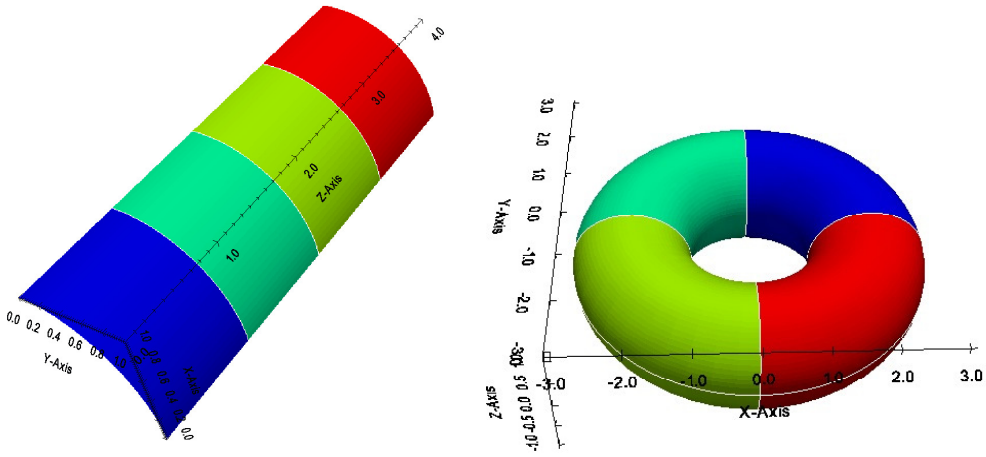

Fig. 4. The computational domain consists of four (4) patches represented in different colours $\Omega_i, i = 1, \ldots, 4$ with corresponding diffusion coefficient $\alpha_i \in \{10^{-4}, 10^4, 10^{-4}, 10^4\}$.

behavior of the dG-IGA scheme with respect to the discrete norm $\|\cdot\|_h$ in Fig.. 5 by successive mesh refinement of ratio $h_i/h_j = 2^q$, where $q = 1, 2, 3$ and $q = 4$ are the refinement level using NURBS of degree $p = 2$ and $p = 4$. We observe the optimal convergence rate as theoretically predicted in Theorem 1 for smooth functions.

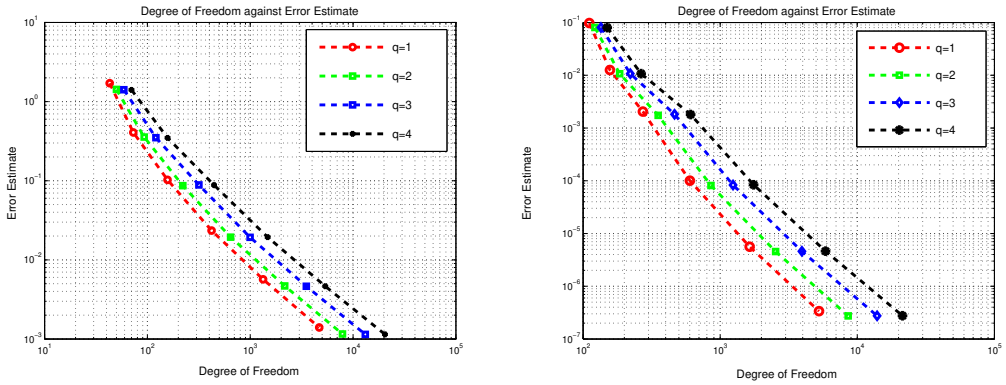

Fig. 5. The convergence rate of mesh refinement levels $q = 1, 2, 3$ and $q = 4$ using B-spline degrees $p = 2$ (left) and $p = 4$ (right) for quarter-cylinder.

6.2 Closed Surface

We consider the closed surface

$$\Omega = \{(x, y) \in (-3, 3)^2, z \in (-1, 1) : \; r^2 = z^2 + (\sqrt{x^2 + y^2} - R^2)\},$$

that is nothing but a torus decomposed into 4 patches, see Fig. 4 (right). The knot vectors describing the NURBS used for the geometrical representation of the patches $\Xi_1 = \{0,0,0,0.25,0.25,0.50,0.50,0.75,0.75,1,1,1\}$ and $\Xi_2 = \{0,0,0,1,1,1\}$. Let us consider the surface Poisson equation with the right-hand side

$$\begin{aligned} f(\phi,\theta) = & \, r^{-2}\left(9\sin(3\phi)\cos(3\theta+\phi)\right) \\ & - \left((R+r\cos(\theta))^{-2}(-10\sin(3\phi)\cos(3\theta+\phi) - 6\cos(3\phi)\sin(3\theta+\phi))\right) \\ & - \left((r(R+r\cos(\theta))^{-1})(3\sin(\theta)\sin(3\phi)\sin(3\theta+\phi))\right), \end{aligned}$$

where $\phi = \arctan(y/x)$, $\theta = \arctan(z/(\sqrt{x^2+y^2}-R))$, $R = 2$ and $r = 1$. The exact solution is given by $u = \sin(3\phi)\cos(3\theta+\phi)$. The functions u and f are chosen such that the zero mean compatibility condition holds. We present the convergence behavior of the dG-IGA scheme with respect to the discrete norm $\|\cdot\|_h$ by successive mesh refinement of ratio $h_i/h_j = 2^q$, where $q = 1,2,3$ and $q = 4$ are the number of mesh refinements using NURBS degrees $p = 2$ and $p = 4$ see Fig. 6. We observe the optimal convergence rate as theoretically predicted in Theorem 1 for smooth functions.

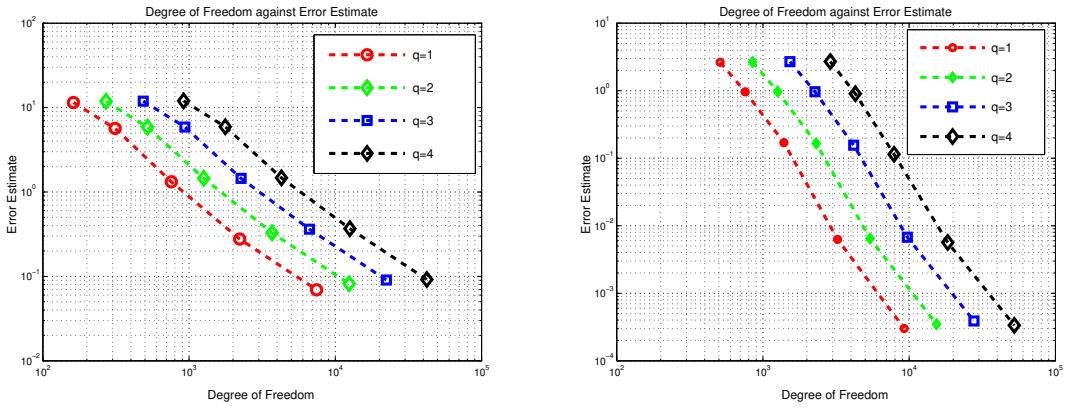

Fig. 6. The convergence rate of mesh refinement levels $q = 1,2,3$ and $q = 4$ using B-spline degree $p = 2$ (left) and $p = 4$ (right).

Conclusion

In this article, we considered the discontinuous Galerkin isogeometric analysis (dG-IGA) for the surface diffusion problem with jumping coefficient and geometrically non-matching meshes. We analyzed the well-posedness and presented *a priori* error estimates. Finally, we presented numerical results confirming the theory presented. In solving the linear system arising from the dG-IGA scheme, we applied the dual-primal discontinuous Galerkin isogeometric tearing and interconnecting method (dG-IETI-DP). This involved a Preconditioned Conjugate Gradient (PCG) algorithm with the scaled Dirichlet preconditioner which is known to be robust with respect to jumping diffusion coefficient. An extension of the results to non-orientable surfaces as well evolving surfaces will be considered in our next article.

Acknowledgement

The author acknowledges the Horizon 2020 Programme (2014-2020) under grant agreement number 678727.

References

1. R. A. Adams and J. J. F. Fournier. *Sobolev Spaces*. Pure and Applied Mathematics 140, Elsevier/Academic Press, second edition, 2008.
2. Y. Bazilevs, L. Beirão da Veiga, J. A. Cottrell, T. J. R. Hughes, and G. Sangalli. Isogeometric analysis: Approximation, stability and error estimates for h-refined meshes. *Comput. Methods Appl. Mech. Engrg.*, 194:4135–4195, 2006.
3. L. Beirão da Veiga, A. Buffa, G. Sangalli, and R. Vázquez. Mathematical analysis of variational isogeometric methods. *Acta Numerica*, 23:157–287, 5 2014.
4. L. Dede and A. Quarteroni. Isogeometric analysis for second order partial differential equations on surfaces. *Comput. Methods Appl. Mech. Engrg.*, 284:807–834, 2015.
5. A. Dedner, P. Madhavan, and B. Stinner. Analysis of the discontinuous Galerkin method for elliptic problems on surfaces. *IMA J. Numer. Anal.*, 33(3):952–973, 2013.
6. D. A. Di Pietro and A. Ern. *Mathematical Aspects of Discontinuous Galerkin Methods*, volume 69 of *Mathématiques et Applications*. Springer-Verlag, Heidelberg, Dordrecht, London, New York, 2012.
7. G. Dziuk and C.M. Elliott. Finite element methods for surface PDEs. *Acta Numerica*, 22:289–396, 2013.
8. J. A. Evans and T. J. R. Hughes. Explicit trace inequalities for isogeometric analysis and parametric hexahedral finite elements. *Numerische Mathematik*, 123(2):259–290, 2013.
9. C. Hofer. Analysis of discontinuous galerkin dual-primal isogeometric tearing and interconnecting methods. *Mathematical Models and Methods in Applied Sciences*, 28(01):131–158, 2018.
10. T. J. R. Hughes, J. A. Cottrell, and Y. Bazilevs. Isogeometric analysis: CAD, finite elements, NURBS, exact geometry and mesh refinement. *Comput. Methods Appl. Mech. Engrg.*, 194:4135–4195, 2005.
11. B. Jüttler, U. Langer, A. Mantzaflaris, S. E. Moore, and W. Zulehner. Geometry + Simulation Modules: Implementing Isogeometric Analysis. *PAMM*, 14(1):961–962, 2014.
12. U. Langer, A. Mantzaflaris, S. E. Moore, and I. Toulopoulos. Multipatch discontinuous galerkin isogeometric analysis. In Bert Jüttler and Bernd Simeon, editors, *Isogeometric Analysis and Applications 2014*, volume 107 of *Lecture Notes in Computational Science and Engineering*, pages 1–32. Springer, 2015.
13. U. Langer and S. E. Moore. Domain decomposition methods in science and engineering xxii. In T. Dickopf, J. M. Gander, L. Halpern, R. Krause, and F. Luca Pavarino, editors, *Domain Decomposition Methods in Science and Engineering XXII*, chapter Discontinuous Galerkin Isogeometric Analysis of Elliptic PDEs on Surfaces, pages 319–326. Springer, Cham, 2016.
14. U. Langer and I. Toulopoulos. Analysis of multipatch discontinuous Galerkin IgA approximations to elliptic boundary value problems. *Computing and Visualization in Science*, 17(5):217–233, 2015.
15. S. E. Moore. *Nonstandard Discretization Strategies In Isogeometric Analysis for Partial Differential Equations*. PhD thesis, Johannes Kepler University, January 2017.
16. S. E. Moore. Discontinuous Galerkin Isogeometric Analysis for the Biharmonic Equation. *Computers & Mathematics with Applications*, 76(4):673 – 685, 2018.
17. K. Shahbazi. An explicit expression for the penalty parameter of the interior penalty method. *Journal of Computational Physics*, 205(2):401 – 407, 2005.
18. J. Wloka. *Partial Differential Equations*. Cambridge University Press, Cambridge, 1987.
19. M. Wu, Y. Wang, B. Mourrain, B Nkonga, and C. Cheng. Convergence rates for solving elliptic boundary value problems with singular parameterizations in isogeometric analysis. *Computer Aided Geometric Design*, 52-53:170 – 189, 2017. Geometric Modeling and Processing 2017.